Equation of state and thermodynamic functions for the fcc soft-core multiple-Yukawa solid and application to fullerenes with compressible molecular radius

Jiu-xun Sun
Department of Applied Physics, University of Electronic Science and Technology, Chengdu 610054, P. R. China
(Received 14 July 2006; revised manuscript received 27 October 2006; published 24 January 2007)

The generalized free volume theory is applied to the soft-core multiple-Yukawa solid, and the hard-core multiple-Yukawa is included in as a special case. The expressions for equation of state and internal energy are derived. The formalism developed is applied to the C_{60}, C_{76}, and C_{84} solids. The effective diameter of C_{60} molecule is taken as the experimental value; the parameters of the double Yukawa (DY) potential for carbon-carbon atoms are determined through fitting the experimental data of cohesive energy, the lattice constant, and the compression curve of C_{60} solid at ambient temperature. The effective diameter of C_{76} and C_{84} molecules are determined through fitting the experimental lattice constants at ambient temperature. The numerical results of C_{60} solid from the soft-core DY potential are in good agreement with the experiments, including the lattice constant and compression curve. The lattice constant versus temperature relationship for C_{76} and C_{84} solids calculated from the DY potential is qualitatively in accordance with experimental data as same as the Girifalco potential. The compression curve of the C_{84} solid calculated from the DY potential deviates from and is softer than the experimental data available. The reason for deviation is discussed, and it is concluded that the influence of compressibility of fullerene molecules to thermophysical quantities is important at high-pressure conditions.

DOI: 10.1103/PhysRevB.75.035424 PACS number(s): 64.10.+h, 64.30.+t, 05.20.−y, 61.48.+c

I. INTRODUCTION

In recent decades, Yukawa fluids have been studied extensively by computer simulations and theories.[1–15] This potential has a screened Coulomb form, and has been applied to many systems, such as the simple fluids,[1–10] colloid fluids,[11–13] liquid metals,[14,15] *et al.* Perhaps the most appealing feature for the Yukawa potential is its analytical availability and simplicity in solving the Ornstern-Zernike (OZ) integral equation under the mean spherical approximation (MSA).[1–10] Apart from the MSA solutions in the r space,[2–6] Tang and Lu proposed a perturbative method to solve the OZ equation for both pure fluids and mixtures.[7–10] They found that the first-order perturbative MSA solution (FMSA) has an outstanding merit in that its results for the one-Yukawa potential are linearly extendible to multiple-Yukawa cases, providing great flexibility to simulate true intermolecular potentials. By mapping the Lennard-Jones (LJ) potential with a two-Yukawa potential, Tang *et al.* developed a MSA theory for the LJ fluid—the basis for studying more complex fluids such as associating chain molecules.[7–10] Note that these studies would have been much more cumbersome had they been performed by the full MSA solution.

However, we notice that the research on Yukawa solids is scarce in contrast to the Yukawa fluids; even the equations of state (EOS) are unavailable both for single and multiple-Yukawa solids. The situation obviously is not suitable for the research of solid-liquid phase transition and phase graph of Yukawa systems. The free volume theory (FVT) has been primitively proposed by Lennard-Jones and Devonshire (LJD) for the LJ liquid.[16] The FVT assumes that all molecules of a system are situated in their equilibrium positions except one, which roams near the center of the cell. The assumption is in more agreement with the practical case of solids; so many works have been done to apply the model to solids. Although the correlation effect has been completely ignored in the FVT, the anharmonic effect can be well taken into account. And Westera and Cowley[17] and Barker[18] have shown that the contribution of correlation effect to thermodynamic quantities is fairly small in conventional cases, except the solids with long-range interaction, such as alkali-halide solids.

The FVT have been demonstrated that can describe satisfactorily the thermophysical properties for the hard-sphere solid,[19] the square-well solid,[20] the fcc Lennard-Jones (LJ) crystal,[17,21] exponential-6 model solid,[22] and sodium chloride,[23] as compared with the Monte Carlo simulations or experiments. Wasserman *et al.*[24] further applied this model to a metallic solid iron, in which the calculated properties are in agreement with available static and shock-wave experimental measurements well. Sun *et al.* extended the FVT to a generalized LJ solid including the quantum modification,[25,26] from which the numerical results are in good agreement with experimental data of solid xenon, both at low and high temperatures.

Recently, Wang *et al.*[27–30] proposed an analytic mean field potential (AMFP) approach, and successfully applied it to many materials. However, this approach was later proven to be equivalent to the FVT, and just is an analytic approximation of FVT.[31] For this reason, we think it is more valuable to directly use the strict FVT than the approximate AMFP, in this case that the equation of state can be derived based on this strict FVT. Recently, we developed a generalized free volume theory (GFVT),[32] through which the equations of state and thermodynamic functions can be derived for most practical potentials. And the GFVT has been applied to a generalized Girifalco C_{60} model solid. In this paper, we will apply the GFVT to the soft-core single- and multiple-Yukawa solids; the results for the multiple-Yukawa solid can be seen as linear combination of single-Yukawa solid and the hard-core multiple-Yukawa is included in as special cases. Considering that other realistic intermolecular potentials can

be mapped by multiple-Yukawa potential, the results in this paper also provide great flexibility to research thermodynamic properties of real solids and solid-liquid phase properties.

In the research of solid C_{60}, Girifalco[33] firstly derived a central potential by using the Lennard-Jones (LJ) (12-6) function, $\varepsilon(r)=B/r^{12}-A/r^6$, to average over the pair of C_{60} cages,

$$\varepsilon(t) = \varepsilon_2\left[\frac{1}{t(t-1)^9}+\frac{1}{t(t+1)^9}-\frac{2}{t^{10}}\right] - \varepsilon_1\left[\frac{1}{t(t-1)^3}+\frac{1}{t(t+1)^3}-\frac{2}{t^4}\right], \quad (1)$$

$$\varepsilon_1 = N_c^2 A/12D^6, \quad \varepsilon_2 = N_c^2 B/90D^{12}, \quad (2)$$

where $t=r/D$, D is the diameter of fullerene cages, and N_c is the number of carbon atoms in a fullerene molecule. Nowadays, the Girifalco potential[33] is most popular in the research of thermodynamic properties of fullerene liquids and solids.[34–59] However, most of these works are computer simulations; most of them are not analytic theories for the complicity of the Girifalco potential. In order to derive the analytic equation of state for the C_{60} fluid, Guérin firstly mimics the Girifalco potential by a double-Yukawa (DY) potential.[57] And Bahaa Khedr *et al.* further studied the properties of C_{60} fluid by using the DY potential.[58] The DY potential has an important merit as integrated on two facing spheres; it yields another DY function. This is fairly convenient for practical applications.

Otherwise, it has been shown that the Girifalco potential is too hard at high pressure.[32,53] We think it is possible to solve the problem by using the DY potential to replace the Girifalco potential. Recently, Abramo *et al.*[53] have explored the influence of atomistic model of C_{60} molecules on the compression effect. However, Ruoff and Ruoff[60,61] have pointed out that the C_{60} molecule is not a stiff sphere but a soft sphere with molecular bulk modulus B_m approximately equal to 820 GPa. Although the value of B_m is fairly large, or the compressibility of the C_{60} molecule is fairly small, we believe that it has important influence to the compression properties of C_{60} solid at high pressures, whereas we have not found any work to research its physical effects up to now. And to the best of our knowledge, we believe that no approach can take the physical effect into account at present, including the computer simulation approaches and theoretical approaches based on the Girifalco potential. The reason can be shown in the formalism developed in the next section, where it can be seen that the compressibility of molecules would make EOS of the system become a differential equation. We must consistently solve pressure, bulk modulus, and thermal expansivity of the system at the same time. Such solving procedure can be implemented just based on the Yukawa-type potential and generalized FVT.

In this paper, we have three main goals. The first goal is to derive expressions of the EOS and internal energy for the soft-core multiple-Yukawa solid by using the GFVT.[32] The formalism for hard-core potential can be included in as special cases. Considering that computer simulations have shown the original Girifalco potential is too hard[32,53] and in the solid state at moderately high pressures, this leads to serious discrepancies with respect to the atomistic simulation results, and to only a poor reproduction of the EOS of real-life C_{60}; our second goal is to apply the DY potential and the formalism developed to fcc C_{60} solid. With the parameters determined by fitting the compression data, lattice constant at 300 K, and the cohesive energy, we can predict the variation of lattice constant versus temperature and all other thermodynamic properties.

Otherwise, we know from Eq. (1) and Eq. (2) that the Girifalco potential can be applied to not only C_{60} but also other fullerenes. And it has been applied to C_{70},[52] C_{76}, and C_{84} (Ref. 59) solids with just two adjustable parameters, N_0 and D, for different fullerenes; the theoretical results are qualitatively in agreement with the experimental data available. Thus our third goal is to apply the DY potential and the formalism developed to other fullerenes, including C_{76} and C_{84}, because some experimental data is available for the two fullerenes.

In Sec. II we present the soft-core multiple-Yukawa potential for fullerenes and some formalism on compressibility of fullerene molecules. In Sec. III, we derive formalism of thermodynamic quantities for the soft-core multiple-Yukawa solid based on the GFVT. In Sec. IV the formalism is applied to fcc C_{60} solid. In Sec. V, the formalism is applied to fcc C_{76} and C_{84} solids. In Sec. VI, the conclusive remark is presented.

II. SOFT-CORE MULTIPLE-YUKAWA POTENTIAL FOR FULLERENES

Supposing the atom-atom interaction is the multiple-Yukawa potential,

$$\phi_c(s) = (\varepsilon_0/s)\sum_{j=1}^{m}(-)^j e^{\lambda_j(1-s)}, \quad (3)$$

with $s=r/\sigma$, ε_0, σ, and λ_i are potential parameters. We have $m=2$ for double-Yukawa potential. The integral over pair of cages yields another multiple-Yukawa potential,[58]

$$\varepsilon(s) = (N_c^2\varepsilon_0/s)\sum_{j=1}^{m} C_j e^{\lambda_j(1-s)}, \quad (4)$$

$$C_j = (-)^j[\sinh(\lambda_j R/\sigma)]^2(\lambda_j R/\sigma)^{-2}, \quad (5)$$

where R is the radius of fullerene cages, N_c is the number of carbon atoms in a fullerene molecule, and $N_c=60$, 76, and 84 for C_{60}, C_{76}, and C_{84} molecules, respectively. The derivatives of $\varepsilon(s)$ with respect to s and R can be derived as

$$\varepsilon'(s) = -(N_c^2\varepsilon_0/s^2)\sum_{j=1}^{m} C_j(1+\lambda_j s)e^{\lambda_j(1-s)}, \quad (6)$$

$$R\frac{\partial\varepsilon(s)}{\partial R} = (N_c^2\varepsilon_0/s)\sum_{j=1}^{m} C_j' e^{\lambda_j}(1-s), \quad (7)$$

$$C_j' = R\frac{\partial C_j}{\partial R} = -2(-)^j[\sinh(\lambda_j R/\sigma)]^2(\lambda_j R/\sigma)^{-2} + 2(-)^j[\sinh(\lambda_j R/\sigma)][\cosh(\lambda_j R/\sigma)](\lambda_j R/\sigma)^{-1}. \quad (8)$$

In terms of Ruoff and Ruoff,[60,61] the dependence of volume of a fullerene molecule with pressure can be expressed as

$$P = B_m\frac{\Delta v_m}{v_m} = B_m\left(\frac{v_{m0}}{v_m} - 1\right), \quad (9)$$

where $v_m = 4\pi R^3/3$ and $v_{m0} = 4\pi R_0^3/3$, the subscript 0 represents the values at zero pressure condition. The pressure dependence of R can be solved as

$$R = R_0(1 + P/B_m)^{-1/3}. \quad (10)$$

Here B_m is the bulk modulus of a fullerene molecule at zero pressure,

$$B_m = 0.449(k_f/R_0) \approx (291/R_0)\ \text{GPa}, \quad (11)$$

and $k_f \approx 67.2$ mdyne/nm is the average force constant of C-C bond.[61] Although Eq. (11) is derived for the C_{60} molecule, we assume it applies to other fullerenes. From Eq. (10), we can derive the pressure dependence of bulk modulus of a fullerene molecule

$$B_{mol} = B_m + P. \quad (12)$$

This means that $\partial B_{mol}/\partial P = 1$, a much lower value as compared to that of graphite $\partial B_{mol}/\partial P = 8.9$ and diamond $\partial B_{mol}/\partial P = 4$, respectively.[61] Thus, we modestly estimate $\partial B_{mol}/\partial P \approx 3$ for fullerenes, and correspondingly modify Eqs. (12), (9), and (10) to the following forms:

$$B_{mol} = B_m + 3P, \quad (13)$$

$$P = \frac{B_m}{3}\left[\left(\frac{v_{m0}}{v_m}\right)^3 - 1\right], \quad (14)$$

$$R = R_0(1 + 3P/B_m)^{-1/9}. \quad (15)$$

The derivatives of R with respect to reduced volume y [defined by Eq. (22)] and temperature T can be derived as

$$\frac{y}{R}\frac{\partial R}{\partial y} = \frac{B}{B_m}\left(1 + \frac{3P}{B_m}\right)^{-1}, \quad (16)$$

$$\frac{T}{R}\frac{\partial R}{\partial T} = -\frac{\alpha T B}{3B_m}\left(1 + \frac{3P}{B_m}\right)^{-1} = -\frac{1}{3}\alpha T\frac{y}{R}\frac{\partial R}{\partial y}. \quad (17)$$

In the derivation of Eq. (17), we have used the thermodynamic relationship

$$\left(\frac{\partial P}{\partial T}\right)_V = \alpha B, \quad (18)$$

where α is the thermal expansivity, and B is the bulk modulus of the solid.

III. EQUATION OF STATE FOR THE SOFT-CORE MULTIPLE-YUKAWA SOLID

In terms of the FVT and GFVT, the free energy can be expressed as[16–32]

$$\frac{F}{NkT} = -\frac{3}{2}\ln(2\pi\mu kT/h^2) + \frac{u(0)}{2kT} - \ln v_f, \quad (19)$$

where μ is the mass of a fullerene molecule, $u(0)$ is the potential energy of a molecule as the lattice is static, v_f is the free volume

$$v_f = 4\pi\int_0^{r_m}\exp\{-[u(r) - u(0)]/kT\}r^2 dr. \quad (20)$$

Here, $u(r)$ is the potential energy of a molecule as it roams from the center to a distance r, $r_m = (3a^3/4\pi\gamma)^{1/3} \approx a/2$ is the Wigner-Seitz radius, a is the nearest-neighbor distance, and γ is the structure constant; for fcc structure, it equals to $\sqrt{2}$.[62]

For simplicity, we introduce the reduced radial coordinate x, the reduced volume y, and the reduced free volume $\bar{v}_f$,

$$x = r/a, \quad x_m = \frac{r_m}{a} \approx \frac{1}{2}, \quad (21)$$

$$y = a/\sigma = (V/V_0)^{1/3}, \quad V = Na^3/\gamma, \quad V_0 = N\sigma^3/\gamma, \quad (22)$$

$$v_f = 4\pi a^3\bar{v}_f = 4\pi\gamma(V/N)\bar{v}_f, \quad (23)$$

where V is the volume of the solid. Considering that $F = F(T,V,R)$, the equation of state and internal energy U can be derived as follows:[32]

$$Z = \frac{PV}{NkT} = -\frac{y}{3}\frac{\partial}{\partial y}\frac{F}{NkT} = \frac{P_c V}{NkT} + \frac{P_f V}{NkT} + \frac{P_r V}{NkT}, \quad (24)$$

$$\frac{P_c V}{NkT} = -\frac{y}{6kT}\left.\frac{\partial u(0)}{\partial y}\right|_{T,R}, \quad (25)$$

$$\frac{P_f V}{NkT} = 1 + \frac{y}{3\bar{v}_f}\left.\frac{\partial \bar{v}_f}{\partial y}\right|_{T,R} \approx 1 - \frac{y\bar{v}_{fb}}{3\bar{v}_f}, \quad (26)$$

where P_c is the cold pressure, P_f is the thermal pressure related to free volume, and P_r is the modification introduced by compressibility of fullerene molecules. With the aid of Eq. (16), we have

$$\frac{P_r V}{NkT} = -\frac{y}{3}\left.\frac{\partial}{\partial y}\frac{F}{NkT}\right|_{T,V} = -\frac{y}{3R}\left.\frac{\partial R}{\partial y}R\frac{\partial}{\partial R}\frac{F}{NkT}\right|_{T,V} = -\frac{B}{3B_m}\left(1 + \frac{3P}{B_m}\right)^{-1}\left[\frac{1}{2kT}R\frac{\partial u(0)}{\partial R} + \frac{v_{fc}}{v_f}\right] \quad (27)$$

By the same procedure, we can derive the expression for the internal energy

$$\frac{U}{NkT} = -T\frac{\partial}{\partial T}\frac{F}{NkT} = \frac{3}{2} + \frac{u(0)}{2kT} + \frac{T}{\bar{v}_f}\frac{\partial \bar{v}_f}{\partial T} - \frac{T}{R}\frac{\partial R}{\partial T}\left.R\frac{\partial}{\partial R}\frac{F}{NkT}\right|_{T,V} = \frac{3}{2} + \frac{u(0)}{2kT} + \frac{\bar{v}_{fa}}{\bar{v}_f} - \alpha T\frac{P_r V}{NkT}. \quad (28)$$

In the derivation of Eqs. (27) and (28), we have used Eqs. (16) and (19), and following relationship

$$R\frac{\partial}{\partial R}\frac{F}{NkT}\bigg|_{T,V} = \frac{1}{2kT}R\frac{\partial u(0)}{\partial R} + \frac{v_{fc}}{v_f}. \quad (29)$$

The expressions for $\bar{v}_f$ and its derivatives with respect to T, y and R are as follows:

$$\bar{v}_f = \int_0^{x_m} \exp\{-[u(x)-u(0)]/kT\}x^2 dx, \quad (30)$$

$$\bar{v}_{fa} = T\frac{\partial}{\partial T}\bar{v}_f = \frac{1}{kT}\int_0^{x_m} \exp\{-[u(x)-u(0)]/kT\}[u(x) - u(0)]x^2 dx, \quad (31)$$

$$\bar{v}_{fb} = -\frac{\partial}{\partial y}\bar{v}_f = \frac{1}{kT}\int_0^{x_m} \exp\{-[u(x)-u(0)]/kT\}\frac{\partial}{\partial y}[u(x) - u(0)]x^2 dx, \quad (32)$$

$$\bar{v}_{fc} = -R\frac{\partial}{\partial R}\bar{v}_f = \frac{1}{kT}\int_0^{x_m} \exp\{-[u(x)-u(0)]/kT\}R\frac{\partial}{\partial R}[u(x) - u(0)]x^2 dx. \quad (33)$$

For the pair potential function $\varepsilon(s)$, the potential energy $u(0)$ can be expressed as

$$u(0) = \sum_{i\neq 0} z_i \varepsilon(\delta_i y), \quad (34)$$

$$\frac{\partial}{\partial y}u(0) = \sum_{i\neq 0} z_i \delta_i \varepsilon'(\delta_i y), \quad (35)$$

where z_i and δ_i are structural constants, and the values for fcc structure have been given in Ref. 62. The potential energy $u(x)$ can be expressed as

$$u(x) = \sum_{i\neq 0} z_i \overline{\varepsilon(s_i)}, \quad (36)$$

$$\frac{\partial}{\partial y}u(r) = \sum_{i\neq 0} z_i \frac{\partial}{\partial y}\overline{\varepsilon(s_i)}, \quad (37)$$

Here $\overline{\varepsilon(s_i)}$ is the average potential over the solid angle, for multiple-Yukawa potential, we have

$$\overline{\varepsilon(s_i)} = \frac{N_c^2 \varepsilon_0}{2\delta_i y^2 x}\sum_{j=1}^{m} C_j \lambda_j^{-1} \cdot \{e^{\lambda_j[1-y(\delta_i - x)]} - e^{\lambda_j[1-y(\delta_i + x)]}\}, \quad (38)$$

$$\frac{\partial}{\partial y}\overline{\varepsilon(s_i)} = -(2y^{-1})\overline{\varepsilon(s_i)} - \frac{N_c^2 \varepsilon_0}{2\delta_i y^2 x}\sum_{j=1}^{m} C_j \times \{(\delta_i - x)e^{\lambda_j[1-y(\delta_i - x)]} - (\delta_i + x)e^{\lambda_j[1-y(\delta_i + x)]}\}. \quad (39)$$

It should be pointed out that in the calculations, we should replace all coefficients C_i by C_i' in $R\partial[u(x)-u(0)]/\partial R$ and related Eqs. (34), (36), and (38). And we also need the expressions for α and B,[32]

$$\alpha = \frac{1}{V}\left(\frac{\partial V}{\partial T}\right)_P = \frac{3}{y}\left(\frac{\partial y}{\partial T}\right)_P = \left[\frac{Z}{T} + \left(\frac{\partial Z}{\partial T}\right)_y\right]\left[Z - \left(\frac{y}{3}\right)\left(\frac{\partial Z}{\partial y}\right)_T\right]^{-1}. \quad (40)$$

$$B = -V\left(\frac{\partial P}{\partial V}\right)_T = -\frac{y}{3}\left(\frac{\partial P}{\partial y}\right)_T = \left(\frac{NkT}{V_d y^3}\right)\left[Z - \left(\frac{y}{3}\right)\left(\frac{\partial Z}{\partial y}\right)_T\right]. \quad (41)$$

The derivatives $(\partial Z/\partial T)_y$ and $(\partial Z/\partial y)_T$ should be calculated numerically. In our program, we have take numerical steps $\Delta T = 0.00001 \times T$ and $\Delta y = 0.00001 \times y$.

From above equations, it can be seen that all thermodynamic quantities are dependent to $R(P)$, $B(P)$, or $\alpha(P)$, including $F(R)$, $P[R(P),B(P)]$ and $U[R(P),B(P),\alpha(P)]$. Thus we are disposing an iteration problem; all physical quantities should be solved consistently. The solving procedure can be realized through following two steps. As a first step, we give initiative values for P, B, and α. At the second step, we can calculate one set of values for all physical quantities. The two steps should be done until the results are consistent within desirable precision. We found the calculations are stable and can converge rapidly. Just about 10 or 20 iterations are needed to reach desirable precision at low and high pressures for calculations presented in this work, respectively.

IV. APPLICATION TO FCC C_{60} SOLID

In this section, we present the numerical results for fcc C_{60} solid by using above formalism. We determine the parameters for the hard-core DY potential in Eq. (4) with incompressible radius $R=R_0$ and by fitting following experimental data, the cohesive energy 175 kJ/mol at 0 K,[55,56] lattice constant 1.417 nm at 300 K, as well as the compression data at 300 K.[63,64] The determined values of parameters are as follows:

$$\lambda_1 = 2.91, \quad \lambda_2 = 8.33, \quad \sigma = 0.366 \text{ nm}, \quad \varepsilon_0 = 73.2 \text{ K}, \quad (42)$$

respectively, and $R_0 = 0.355$ nm. We compare the DY potential with Girifalco potential for C_{60} molecules with radius $R=R_0$ in Figure 1. The figure shows that the difference of well depth and equilibrium distance between the two potentials is small; the curve of the DY potential is flatter, and the repulsion is softer than the Girifalco potential.

The calculated thermodynamic properties at zero pressure and different temperatures by using the DY potential with

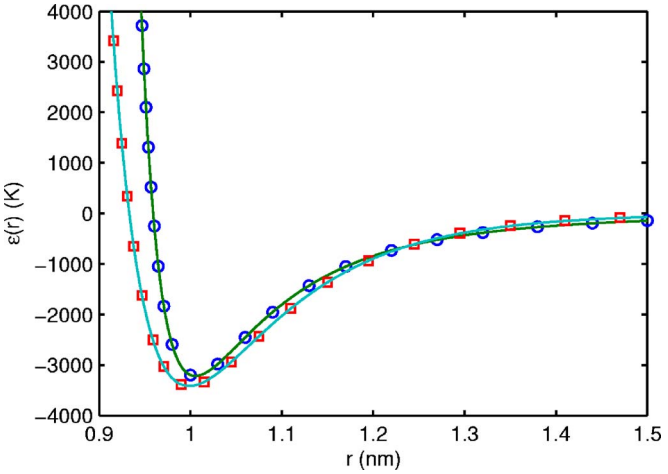

FIG. 1. (Color online) Comparison of original Girifalco potential (line with circles) with the DY potential taking constant $R=R_0$ (line with squares) proposed in this work.

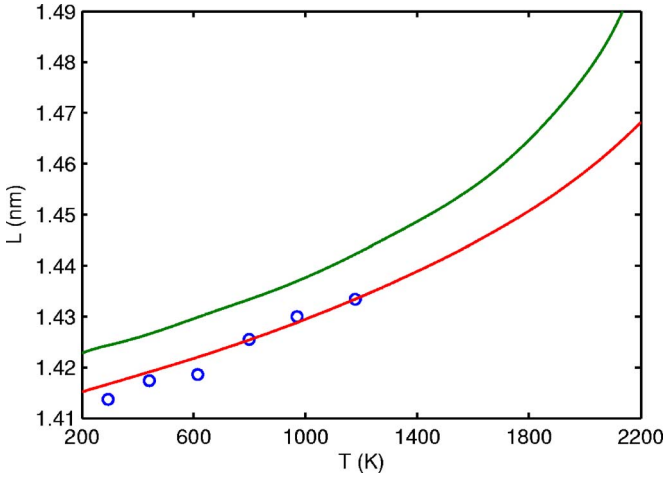

FIG. 2. (Color online) Comparison of lattice constant $L(=\sqrt{2}a)$ versus temperature relationship at zero pressure: Upper line: GFVT results for original Girifalco potential; Lower line: GFVT results for the soft-core DY potential; circles: experimental data from Ref. 65.

incompressible (hard-core) or compressible (soft-core) molecular radius R_0 or R are listed in Table I. The table shows that the compressibility of molecular radius has little influence to physical quantities at zero pressure. The spinodal point T_s is the temperature satisfying the condition, $B_T(T_s)=0$.[55,56] The system is instable for temperature above T_s. For the Girifalco potential, molecular dynamics (MD) simulations performed by Cheng *et al.*[51] and Abramo and Caccamo[52] give $T_s=2320$ K, our GFVT calculations give $T_s=2605$ K. Figures 2–6 present the GFVT results of thermodynamic properties of fcc C_{60} solid calculated by using the DY potential with incompressible or compressible molecular radius R_0 or R. For Figure 2, the available experimental data and the results from the Girifalco potential have been presented for comparison.

Figure 2 shows that the agreement of calculated variation of lattice constant versus temperature with experiment[65] is fairly bad for the Girifalco potential, and satisfactory for the soft-core DY potential. In the figure, the difference between two sets of lattice constants for the hard and soft-core DY potentials as listed in Table I is invisible, and just the lattice

TABLE I. Properties of the fcc phase of C_{60}: the lattice constant $L=(\sqrt{2}a)$, a in nm, linear thermal expansion coefficient α in 10^{-5} K^{-1}, the heat capacity C_V in kJ mol^{-1} K^{-1}, and the bulk modulus B_T in kbar. The values in the first and second lines have been calculated with the FVT combining the hard-core and soft-core DY potentials, respectively.

T	200	300	400	500	600	800	1000	1200	1400	1600
L	1.4154	1.4170	1.4186	1.4203	1.4220	1.4257	1.4297	1.4341	1.4390	1.4446
	1.4152	1.4168	1.4184	1.4201	1.4218	1.4255	1.4295	1.4339	1.4389	1.4444
α	1.0933	1.1280	1.1653	1.2056	1.2493	1.3487	1.4684	1.6158	1.8026	2.0485
	1.0886	1.1232	1.1604	1.2005	1.2441	1.3431	1.4624	1.6092	1.7952	2.0401
B_T	89.603	85.795	82.019	78.274	74.558	67.211	59.968	52.822	45.761	38.769
	89.351	85.583	81.844	78.132	74.447	67.154	59.955	52.843	45.807	38.833
C_V	24.628	24.476	24.321	24.163	24.001	23.670	23.324	22.958	22.568	22.146
	24.636	24.487	24.334	24.179	24.021	23.695	23.353	22.991	22.604	22.185

T	1800	2000	2200	2400	T_s
L	1.4510	1.4586	1.4683	1.4820	1.5230
	1.4508	1.4584	1.4681	1.4818	1.5229
α	2.3899	2.9040	3.7930	5.8641	460.19
	2.3800	2.8918	3.7763	5.8352	403.42
B_T	31.824	24.886	17.876	10.569	0.1029
	31.897	24.961	17.943	10.621	0.1175
C_V	21.680	21.150	20.520	19.694	17.651
	21.720	21.191	20.560	19.731	17.677

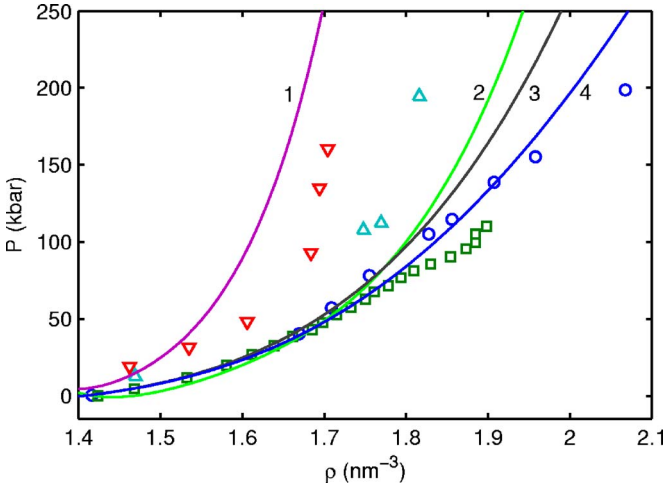

FIG. 3. (Color online) Comparison of isothermals of solid C_{60} calculated in this work by using original Girifalco potential (line 1), the modified Girifalco potential in Ref. 32 (line 2), the hard-core DY potential (line 3), and the soft-core DY potential (line 4) with experiments at 300 K. The symbols refer to experimental data, by Horikawa *et al.* in Ref. 63 (squares), and by Duclos *et al.* in Ref. 64 at 20 GPa (circles), 10 GPa (up triangles), and 4 GPa (down triangles), respectively.

constants of the soft-core DY potential are plotted for clarity. Figure 3 shows that the compression curve for the original Girifalco potential is too hard as compared with experiments;[63,64] as having been shown by Refs. 32 and 53, the DY potential gives much softer and improved compression curve. In Ref. 32, we have proposed a modified Girifalco potential based on the LJ (7-6) potential, $\varepsilon(r)=A/r^7 - B/r^6$, with parameters determined from the same input experimental dataset as the DY potential. In Figure 3, we also plotted the compression curve calculated from the modified Girifalco potential. It can be seen that the DY potential gives better results than the modified Girifalco potential. The

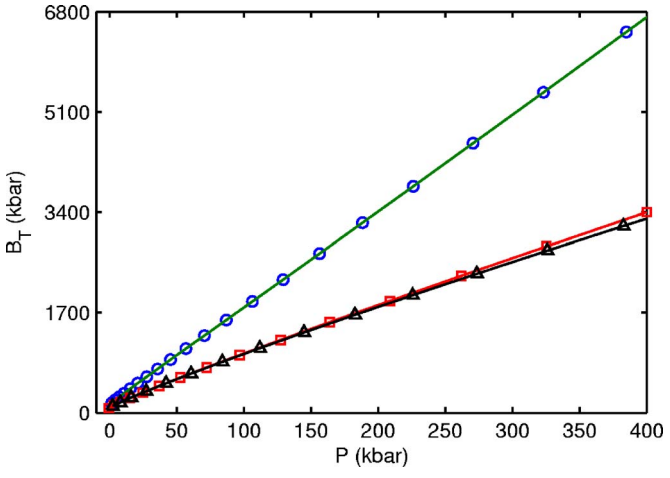

FIG. 4. (Color online) Variation of the bulk modulus (kbar) versus pressure calculated in this work at 300 K, and by using the original Girifalco potential (line with circles), the hard-core DY potential (line with squares), and the soft-core DY potential (line with triangles), respectively.

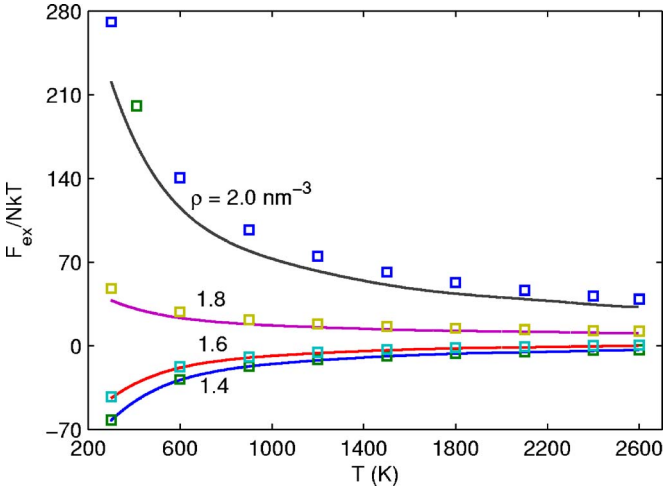

FIG. 5. (Color online) Excess free energy as function of temperature calculated for several densities ρ calculated by using the GFVT with the hard-core and soft-core DY potentials. The squares represent results of the hard-core DY potential for ρ=2.0, 1.8, 1.6, and 1.4 nm^{-8} from up to down, respectively. The lines represent results of the soft-core DY potential for the same densities, respectively.

modified Girifalco potential tends to be too soft in the middle pressure region, and yet too hard as compared with the latest experimental data. Comprehensively, the hard-core DY potential gives better results in low and middle high-pressure regions than the modified Girifalco potential. The influence of compressibility of molecular radius to the compression curve is not evident at low pressure conditions, and enlightened at high-pressure condition. The soft-core DY potential gives the best results as compared with the latest experimental data in all of low-, middle-, and high-pressure regions.

Figure 4 gives the variation of bulk modulus B_T versus pressure relationship. The figure shows that B_T is a linear increasing function of pressure, but the slope is fairly large and the increase is fast. The difference of B_T is small at low density and increases at high density. The value of B_T for the

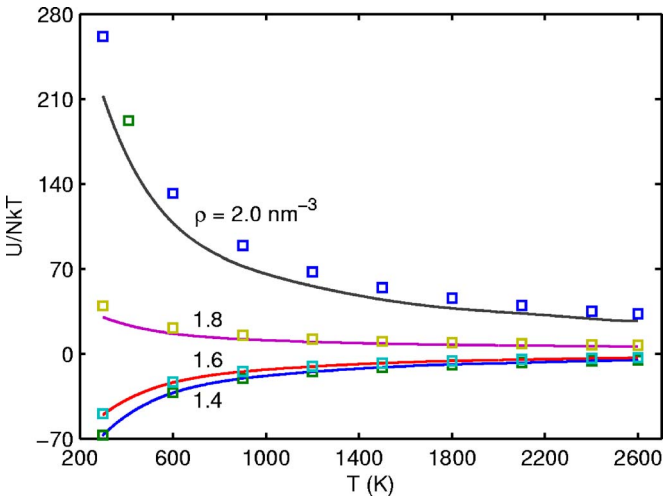

FIG. 6. (Color online) The same as for Figure 5, but for internal energy.

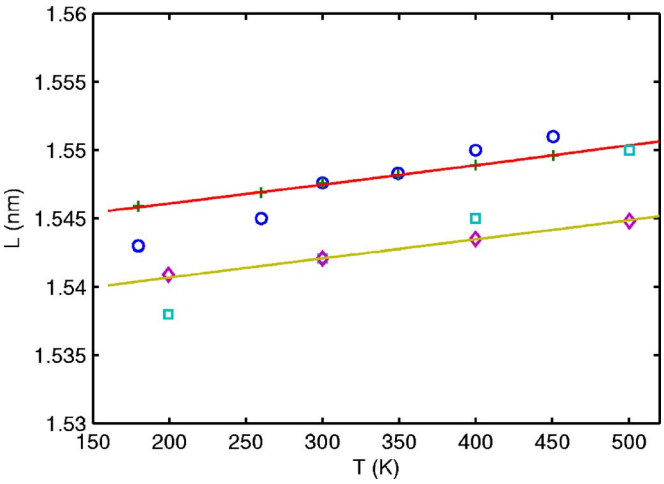

FIG. 7. (Color online) Lattice constant of C_{60} solid versus temperature relationship. Upper and lower lines: results calculated by using the GFVT and the soft-core DY potential with R_0 =0.40103 nm and 0.39915 nm, respectively; pluses and diamonds: MD results of Ref. 59 by using the Girifalco potential with the diameter D=0.7977 nm and 0.7949 nm, respectively; Circles and squares: experimental data in Refs. 66 and 67, respectively.

DY potential at high pressure is far smaller than that for the Girifalco potential. This means the model solid of fcc C_{60} with the DY potential is far softer than that with the Girifalco potential. It also can be shown that the influence of compressibility of molecular radius with bulk modulus is fairly small.

In Figures 6 and 7, we plotted the reduced excess free energy F_{ex}/NkT and reduced internal energy U/NkT versus temperature relationships at four densities. The reduced excess free energy is defined as follows:

$$\frac{F_{ex}}{NkT} = \frac{F}{NkT} + \frac{3}{2}\ln(2\pi\mu\sigma^2 kT/h^2). \tag{43}$$

The two figures show that both F_{ex}/NkT and U/NkT are increasing functions of temperature at low densities, and are decreasing functions of temperature at high densities. Both quantities have the convergence tendency at high temperatures. U/NkT tends to a constant 3/2, yet F_{ex}/NkT does not tend to a constant but to a weakly density dependent value. The influence of the compressibility of molecular radius to F_{ex}/NkT is evident at high densities and not at low densities. The hard-core DY potential gives larger values of F_{ex}/NkT and U/NkT than the soft-core DY potential at high densities. And the two potentials give almost the same values at low densities. Considering that phase properties and physics-chemical properties are sensitive to the potential form, evident difference would exist between the softer and harder potentials. And we think that in order to describe physical properties of materials with heavy molecular weight at high-pressure conditions, the inclusion of compressibility of molecules is important.

V. APPLICATION TO FCC C76 AND C84 SOLIDS

In terms of the derivation of DY potential in Eq. (4), it is clear that the DY potential can be applied to other fullerenes with the same four parameters in Eq. (42) and different N_c and R_0 for different fullerenes. Two different values of the lattice constant of C_{76} fullerite are available from x-ray experiments,[66,67] and corresponding to them one can determine two different "effective" diameters. As far as the determination of an effective diameter of C_{84} is concerned, we follow a similar procedure as for C_{76}, by making reference to recent experimental determinations of the lattice constant.[68,69] The final R_0 values and the experimental lattice constants of C_{76} and C_{84}, used for the fit, are reported in Table II.

Saito *et al.*[70] assume that the radius of a fullerene molecule is proportional to the square root of the surface area of a molecule (or the number of carbon atoms constituting the fullerene), and they define the following expression as the radius of the fullerene molecule:

$$R_0 = 0.355 \times \sqrt{N_c/60}. \tag{44}$$

The table shows that the fitted R_0 values are in good agreement with the theoretical values calculated from Eq. (44). In the table, we also list the values of spinodal point T_s and the sublimation heat ΔH at some reference temperatures. From the table and results for C_{60}, we know that the values of T_s have the following sequence: $T_s(C_{84}) > T_s(C_{76}) > T_s(C_{60})$. This means that the fullerene solids can keep stable at higher

TABLE II. Fitted and theoretical values of the effective radius R_0 of C_{76} and C_{84} molecules for the soft DY potential; experimental data (Refs. 66–69) of lattice spacing $L(=\sqrt{2}a)$ at a reference temperature T_{ref} used to determine the effective radius; the spinodal temperatures T_s calculated by using the soft DY potential; and the calculated and experimental values (Refs. 69 and 71) of sublimation heat ΔH at a temperature.

Matters	Ref.	T_{ref} (K)	L_{exp} (nm)	R_0 (nm)		T_s (K)	ΔH (kJ/mol)		
				fitting	Eq. (44)		Calculated	Experimental	Ref.
C_{60}	53	—	—	0.355	0.355	2605.4	167.5	168.0 (300 K)	53
C_{76}	66	297	1.5475	0.40103	0.39954	2959.2	193.5	206±4	69
C_{76}	67	297	1.5421	0.39915		2999.0	196.1	(298 K)	
C_{84}	68	230	1.5894	0.41617	0.420004	3252.9	214.1	214±6	71
C_{84}	69	300	1.6000	0.41956		3178.7	209.2	(300 K)	

TABLE III. The same as for Table I, but for C_{76} with R_0=0.39915 nm (first lines) and 0.40103 nm (second lines), respectively.

T	200	300	400	500	600	800	1000	1200	1400	1600
L	1.5461	1.5475	1.5489	1.5504	1.5519	1.5550	1.5584	1.5621	1.5661	1.5705
	1.5407	1.5421	1.5435	1.5449	1.5464	1.5495	1.5528	1.5564	1.5603	1.5646
α	0.8732	0.8972	0.9229	0.9504	0.9798	1.0454	1.1220	1.2129	1.3228	1.4588
	0.8638	0.8873	0.9123	0.9390	0.9675	1.0312	1.1053	1.1930	1.2985	1.4283
B_T	93.406	89.978	86.572	83.188	79.825	73.160	66.572	60.055	53.602	47.205
	95.093	91.651	88.232	84.834	81.458	74.766	68.150	61.604	55.123	48.698
C_V	24.669	24.539	24.405	24.269	24.131	23.847	23.552	23.244	22.920	22.575
	24.673	24.544	24.413	24.279	24.142	23.863	23.573	23.270	22.952	22.614

T	1800	2000	2200	2400	2600	2800	T_s
L	1.5753	1.5809	1.5873	1.5950	1.6049	1.6197	1.6544
	1.5694	1.5747	1.5809	1.5883	1.5976	1.6109	1.6491
α	1.6321	1.8624	2.1867	2.6863	3.5896	5.9748	334.50
	1.5928	1.8092	2.1098	2.5629	3.3489	5.2008	354.20
B_T	40.854	34.531	28.212	21.850	15.345	8.3930	0.1199
	42.319	35.971	29.631	23.258	16.766	9.9186	0.1139
C_V	22.204	21.799	21.348	20.830	20.201	19.342	17.642
	22.251	21.857	21.419	20.920	20.322	19.534	17.641

temperature for fullerene with heavier molecules. The table also shows that the calculated values of ΔH are in good agreement with the experimental data[69,71] for all fullerenes considered in this work.

We firstly calculate the thermodynamic properties of C_{76} and C_{84} at zero pressure and from 200 K to T_s by using the soft-core DY potential and two different effective fullerene diameters in Table II. The results are listed in Tables III and IV. The fcc lattice constants for C_{76} and C_{84} in the temperature ranges 180–500 K and 150–350 K are shown in Figures 7 and 8, respectively. In the two figures, we also plotted the MD results by using the Girifalco potential from Micali *et al.*[59] It is shown that the results from the soft-core DY and Girifalco potentials are almost identical, and both are quali-

TABLE IV. The same as for Table I, but for C_{84} with R_0=0.41617 nm (first lines) and 0.41956 nm (second lines), respectively.

T	200	300	400	500	600	800	1000	1200	1400	1600
L	1.5890	1.5902	1.5915	1.5928	1.5942	1.5970	1.6000	1.6032	1.6066	1.6104
	1.5987	1.5999	1.6013	1.6026	1.6040	1.6069	1.6100	1.6133	1.6169	1.6207
α	0.7694	0.7886	0.8088	0.8304	0.8533	0.9037	0.9616	1.0287	1.1077	1.2023
	0.7838	0.8038	0.8250	0.8475	0.8716	0.9247	0.9859	1.0572	1.1417	1.2435
B_T	100.39	97.068	93.758	90.468	87.196	80.706	74.285	67.927	61.628	55.383
	97.354	94.046	90.758	87.490	84.240	77.796	71.421	65.110	58.859	52.661
C_V	24.692	24.575	24.454	24.331	24.206	23.951	23.687	23.413	23.127	22.826
	24.687	24.566	24.442	24.316	24.188	23.926	23.655	23.373	23.078	22.766

T	1800	2000	2200	2400	2600	2800	3000	T_s
L	1.6145	1.6190	1.6240	1.6298	1.6367	1.6452	1.6567	1.6982
	1.6250	1.6297	1.6351	1.6413	1.6487	1.6581	1.6717	1.7074
α	1.3178	1.4628	1.6512	1.9083	2.2857	2.9094	4.2179	836.51
	1.3690	1.5285	1.7392	2.0336	2.4819	3.2745	5.2427	349.80
B_T	49.183	43.019	36.878	30.738	24.564	18.284	11.723	0.0454
	46.507	40.388	34.288	28.181	22.024	15.723	9.0066	0.1076
C_V	22.507	22.166	21.795	21.386	20.924	20.379	19.685	17.610
	22.436	22.080	21.692	21.260	20.766	20.171	19.373	17.627

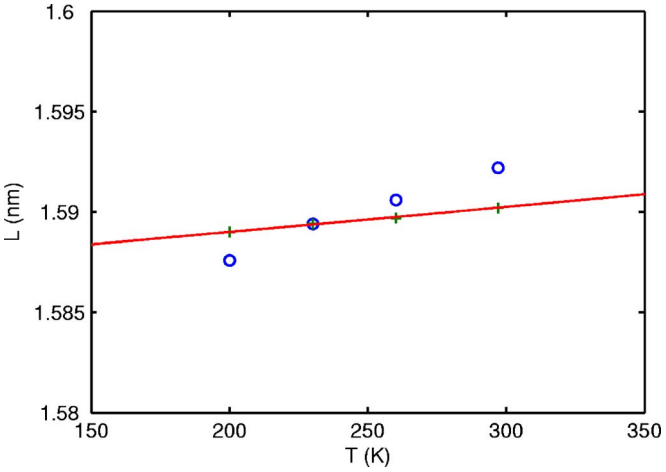

FIG. 8. (Color online) Lattice constant of solid versus temperature relationship. Line: results calculated by using the GFVT and the soft-core DY potential with R_0=0.41617 nm; pluses: MD results of Ref. 59 by using the Girifalco potential the diameter D =0.83075 nm; circles: experimental data in Ref. 68.

tatively in agreement with the experimental data.

In Figure 9, we plotted the variation of bulk modulus B_T of C_{76} and C_{84} versus pressure relationship calculated from the soft-core DY and hard-core Girifalco potentials. The comparison of Figure 9 with Figure 4 shows that the situation is almost the same. It is shown that the difference of values of B_T is small between C_{76} and C_{84} as the same potential is used, but is large between the different Girifalco and DY potentials for the same fullerenes.

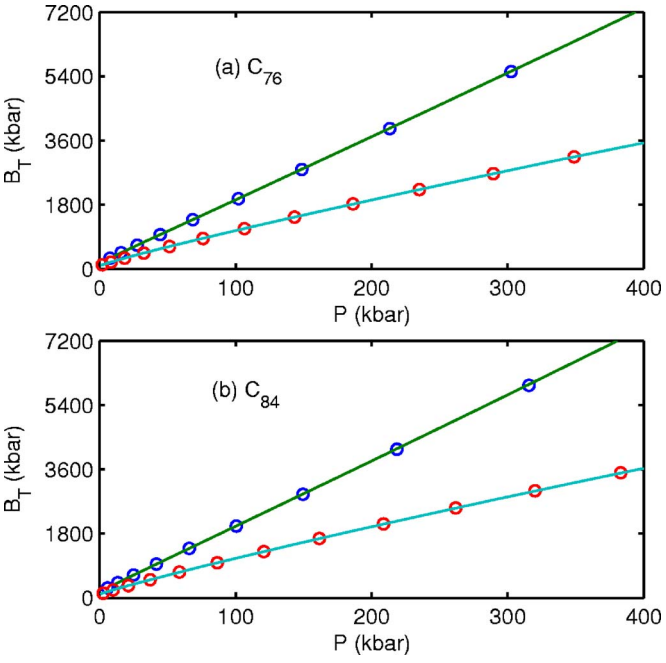

FIG. 9. (Color online) Variation of the bulk modulus (kbar) for C_{76} (a) and C_{84} (b) solids at 300 K versus pressure calculated in this work by using the original Girifalco potential (upper lines and circles) and the soft-core DY potential (lower lines and circles), respectively; circles: results with large values of diameter in Ref. 59 or radius in Table II; lines: results with small values of diameter in Ref. 59 or radius in Table II.

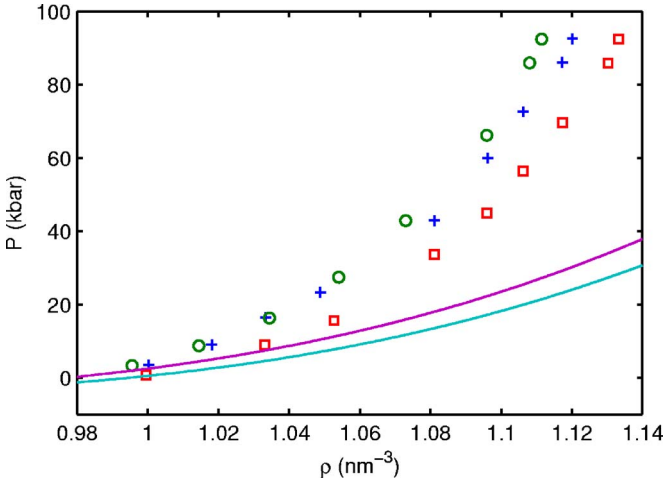

FIG. 10. (Color online) Comparison of isothermals of solid C_{84} at 300 K calculated in this work by using original Girifalco potential (circles and squares with the diameter D=0.83075 nm and 0.83591 nm, respectively), and the soft-core DY potential (upper and lower lines with R_0=0.41617 nm and 0.41956 nm, respectively) with experiments in Ref. 69 by Brunetti *et al.* (pluses).

In Figure 10, the results for compression curves of C_{84} solid from the soft-core DY potential by us and from Girifalco potential by Micali *et al.*[59] are compared with experiment.[69] The figure shows that the results deduced from the Girifalco potential by Micali *et al.*[59] is satisfactorily in agreement with the experimental data, yet the results from the soft-core DY potential evidently deviate from the experimental data. Although the compression curve of the C_{84} solid obtained from the Girifalco potential is in accordance with experiment, we do not think the Girifalco potential is superior to the DY potential because the former is too hard for C_{60} solid, as shown in Figure 3. This implies that some discrepancy exists between the theory and experiment. Noting that the experimental data for C_{60} solid[63,64] measured in the narrow pressure ranges tends to be too hard, the data measured in the wide pressure ranges is much softer (as shown in Figure 3), and the compression data of C_{84} has been measured in the narrow pressure range.[69] We think that most probably the experimental compression curve of C_{84} solid shown in Figure 10 also is too hard. In order to solve the discrepancy, we need more work both from theoretical and experimental aspects.

VI. CONCLUSION

In summary, the equation of state and the internal energy for the soft-core multiple-Yukawa solid have been derived by using the GFVT.[32] The formalism for the hard-core multiple-Yukawa solid can be included in this paper as special cases. The formalism developed is applied to the C_{60}, C_{76}, and C_{84} solids. With the effective diameter of C_{60} molecule taken as the experimental value, the parameters of the DY potential for carbon-carbon atoms are determined through fitting the experimental data of cohesive energy, lattice constant, and

compression curve of C_{60} solid at ambient temperature. The effective diameter of C_{76} and C_{84} molecules are determined through fitting the experimental lattice constants at ambient temperature. The difference of equilibrium distance and well depth for C_{60} molecules between the DY potential and the Girifalco potential is small, but the repulsion of the DY potential is softer than the Girifalco potential. The calculated variation of lattice constant versus temperature relationship and compression curve for C_{60} solid are in good agreement with experimental data available. However, the calculated variations of lattice constant versus temperature relationship for C_{76} and C_{84} solids are almost identical between the DY and Girifalco potentials, and are merely qualitatively in agreement with experimental data available. The agreement of compression curve of C_{60} solid calculated from the soft-core DY potential with the latest experimental data is the best one as compared with the hard-core DY potential and Girifalco potentials, whereas the compression curve of C_{84} solid calculated from the DY potential evidently deviates from the experimental data available in the low-pressure range. Some discrepancy exists between theory and experiment. It is proposed that more theoretical and experimental researches are needed to solve the discrepancy.

ACKNOWLEDGMENT

This work was supported by the Support Programs for Academic Excellence of Sichuan Province of China under Grant No. 06ZQ026-010, the Education Ministry of China under Grant No. NCET-05-0799, and UESTC under Grant No. 23601008.

[1] J. X. Sun, Phys. Rev. E **68**, 061503 (2003).
[2] Y. Z. Lin, Y. G. Li, J. F. Lu, and W. Wu, J. Chem. Phys. **117**, 10165 (2002).
[3] D. Henderson, L. Blum, and J. P. Noworyta, J. Chem. Phys. **102**, 4973 (1995).
[4] J. N. Herrera, H. Ruiz-Estrada, and L. Blum, J. Chem. Phys. **104**, 6327 (1996).
[5] L. Blum and J. N. Herrera, Mol. Phys. **96**, 821 (1999).
[6] L. Blum and M. Ubriaco, Mol. Phys. **98**, 829 (2000).
[7] Y. Tang, Y. Z. Lin, and Y. G. Li, J. Chem. Phys. **122**, 184505 (2005).
[8] Y. Tang, Mol. Phys. **100**, 1033 (2002).
[9] Y. Tang and J. Wu, Phys. Rev. E **70**, 011201 (2004).
[10] Y. Tang, J. Chem. Phys. **121**, 10605 (2004).
[11] J. Wu, Y. Liu, W. R. Chen, J. Cao, and S. H. Chen, Phys. Rev. E **70**, 050401(R) (2004).
[12] M. Bouaskarne, S. Amokrane, and C. Regnaut, J. Chem. Phys. **111**, 2151 (1999).
[13] M. Hasegawa, J. Chem. Phys. **108**, 208 (1998).
[14] M. S. S. Brooks, J. Phys.: Condens. Matter **13**, L469 (2001).
[15] I. L. McLaughlin and K. N. Khanna, J. Non-Cryst. Solids **117**, 100 (1990).
[16] J. E. Lennard-Jones and A. F. Devonshire, Proc. R. Soc. London, Ser. A **163**, 53 (1937); J. E. Lennard-Jones and A. F. Devonshire, *ibid.* **165**, 1 (1938); J. E. Lennard-Jones and A. F. Devonshire, *ibid.* **169**, 317 (1939); J. E. Lennard-Jones and A. F. Devonshire, *ibid.* **170**, 464 (1939).
[17] K. Westera and E. R. Cowley, Phys. Rev. B **11**, 4008 (1975).
[18] J. A. Barker, Proc. R. Soc. London, Ser. A **230**, 390 (1955); J. A. Barker, *ibid.*, **237**, 63 (1956). J. A. Barker, *ibid.* **240**, 265 (1957).
[19] Z. W. Salsburg and W. W. Wood, J. Chem. Phys. **37**, 798 (1962).
[20] B. J. Alder, J. Chem. Phys. **31**, 1666 (1959).
[21] F. H. Ree and A. C. Holt, Phys. Rev. B **8**, 826 (1973).
[22] A. C. Holt and M. Ross, Phys. Rev. B **1**, 2700 (1970).
[23] E. R. Cowley, J. Gross, Z. X Gong, and G. K. Horton, Phys. Rev. B **42**, 3135 (1990).
[24] E. Wasserman, L. Stixrude, and R. E. Cohen, Phys. Rev. B **53**, 8296 (1996).
[25] J. X. Sun, H. C. Yang, Q. Wu, and L. C. Cai, J. Phys. Chem. Solids **63**, 113 (2002).
[26] J. X. Sun, Physica B, **315**, 101 (2002).
[27] Y. Wang, D. Chen, and X. Zhang, Phys. Rev. Lett., **84**, 3220 (2000).
[28] Y. Wang and L. Li, Phys. Rev. B, **62**, 196 (2000).
[29] L. Li and Y. Wang, Phys. Rev. B, **63**, 245108 (2001).
[30] Y. Wang, R. Ahuja, and B. Johansson, Phys. Rev. B **65**, 014104 (2001).
[31] Jiu-xun Sun, Ling-cang Cai, Qiang Wu, and Fuqian Jing, Phys. Rev. B **71**, 024107 (2005).
[32] J. X. Sun, L. Cai, Q. Wu, and F. Jing, Phys. Rev. B **73**, 155431 (2006).
[33] L. A. Girifalco, J. Phys. Chem. **96**, 858 (1992).
[34] K. Ohno, Y. Maruyama, and Y. Kawazoe, Phys. Rev. B **53**, 4078 (1996).
[35] A. Cheng, M. L. Klein, and C. Caccamo, Phys. Rev. Lett. **71**, 1200 (1993).
[36] C. Rey, L. J. Gallego, and J. A. Alonso, Phys. Rev. B **49**, 8491 (1994).
[37] M. H. J. Hagen, E. J. Meijer, G. C. A. M. Mooij, D. Frenkel, and H. N. W. Lekkerkerker, Nature **365**, 425 (1993).
[38] M. H. J. Hagen and D. Frenkel, J. Chem. Phys. **101**, 4093 (1994).
[39] C. Caccamo, D. Costa, and A. Fucile, J. Chem. Phys. **106**, 255 (1997).
[40] D. Costa, G. Pellicane, M. C. Abramo, and C. Caccamo, J. Chem. Phys. **118**, 304 (2003).
[41] M. Hasegawa and K. Ohno, J. Chem. Phys. **111**, 5955 (1999).
[42] M. Hasegawa and K. Ohno, J. Chem. Phys. **113**, 4315 (2000).
[43] M. Hasegawa and K. Ohno, J. Phys.: Condens. Matter **9**, 3361 (1997).
[44] L. Mederos and G. Navascu'es, Phys. Rev. B **50**, 1301 (1994).
[45] M. Hasegawa and K. Ohno, Phys. Rev. E **54**, 3928 (1996).
[46] C. Caccamo, Phys. Rev. B **51**, 3387 (1995).
[47] M. Tau, A. Parola, D. Pini, and L. Reatto, Phys. Rev. E **52**, 2644 (1995).
[48] H. Guerin, J. Phys.: Condens. Matter **10**, L527 (1998).
[49] M. Khedr, M. S. Al-Busaidy, and S. M. Osman, J. Phys.: Condens. Matter **17**, 4411 (2005).

[50] D. Costa, G. Pellicane, C. Caccamo, E. Scholl-Paschinger, and G. Kahl, Phys. Rev. E **68**, 021104 (2003).
[51] A. Cheng, M. L. Klein, and C. Caccamo, Phys. Rev. Lett. **71**, 1200 (1993).
[52] M. C. Abramo and C. Caccamo, J. Phys. Chem. Solids **57**, 1751 (1996).
[53] M. C. Abramo, C. Caccamo, D. Costa, G. Pellicane, and R. Ruberto, Phys. Rev. E **69**, 031112 (2004).
[54] L. A. Girifalco, Phys. Rev. B **52**, 9910 (1995).
[55] V. I. Zubov, N. P. Tretiakov, J. F. Sanchez, and A. A. Caparica, Phys. Rev. B **53**, 12080 (1996).
[56] V. I. Zubov, J. F. Sanchez-Ortiz, J. N. Teixeira Rabelo, and I. V. Zubov, Phys. Rev. B **55**, 6747 (1997).
[57] H. Guérin, J. Phys.: Condens. Matter **10**, L527 (1998).
[58] M. Bahaa Khedr, M. S. Al-Busaidy, and S. M. Osman, J. Phys.: Condens. Matter **17**, 4411 (2005).
[59] F. Micali, M. C. Abramo, and C. Caccamo, J. Phys. Chem. Solids **64**, 319 (2003).
[60] R. S. Ruoff and A. L. Ruoff, Nature **350**, 663 (1991).
[61] R. S. Ruoff and A. L. Ruoff, Appl. Phys. Lett. **59**, 1553 (1991).
[62] Nan-xian Chen, Zhao-dou Chen, and Yu-chuan Wei, Phys. Rev. E **55**, R5 (1997).
[63] T. Horikawa, T. Kinoshita, K. Suito, and A. Onodera, Solid State Commun. **114**, 121 (2000).
[64] S. Duclos, K. Brister, R. C. Haddon, A. R. Kortan, and F. A. Theil, Nature (London) **351**, 380 (1991).
[65] J. F. Fischer and P. A. Heiney, J. Phys. Chem. Solids **54**, 1725 (1993).
[66] H. Kawada, Y. Fujii, H. Nakao, Y. Murakami, T. Watanuki, H. Suematsu, K. Kikuchi, Y. Achiba, and I. Ikemoto, Phys. Rev. B **51**, 8723 (1995).
[67] H. Nakao, Y. Fujii, T. Watanuki, K. Ishii, H. Suematsu, H. Kawada, Y. Murakami, K. Kikuchi, Y. Achiba, and Y. Maniwa, J. Phys. Soc. Jpn. **67**, 4117 (1998).
[68] S. Margadonna, C. M. Brown, T. J. S. Dennis, A. Lappas, P. Pattison, K. Prassides, and H. Shinohara, Chem. Mater. **10**, 1742 (1998).
[69] B. Brunetti, G. Gigli, V. Piacente, and P. Scardala, J. Phys. Chem. B **101**, 10715 (1997).
[70] Y. Saito, T. Yoshikawa, N. Fujimoto, and H. Shinohara, Phys. Rev. B **48**, 9182 (1993).
[71] V. Piacente, C. Palchetti, G. Gigli, and P. Scardala, J. Phys. Chem. A **101**, 4303 (1997).